

## Study the effect of adding silver nanoparticles on the electrical properties of the binary system mixture of compounds with liquid crystal properties

Osama A. Ibrahim<sup>1</sup>, Emaad Al-Tikrity<sup>1</sup>, Issam A. Al latif<sup>2</sup>, Hanah Kaan Salih<sup>1</sup>

<sup>1</sup> Department of Chemistry, College of Science, University of Tikrit, Tikrit, Iraq

<sup>2</sup> Department of Chemistry, College of Education, Ibn al-Haytham, University of Baghdad, Baghdad, Iraq

### Abstract

The importance of the compounds which have liquid crystalline properties comes from its uses in a lot of practical applications; therefore the study of its electrical properties and the effect of the nanoparticles on its electrical properties are considered one of the most important things.

In this study many of organic compounds have been prepared and then diagnosed by using the IR spectroscopy (FT-IR), and the differential scanning calorimeter (DSC) and also the Polarized light microscopy.

And then we selected two compounds that possess liquid crystalline properties and we made a combination of the bilateral system, and we got the less temperature at a concentration of (53% A). This combination of the bilateral system diagnosed by using the differential scanning calorimeter (DSC) and Polarized light microscopy.

Silver nanoparticles have been prepared and then diagnosed by x-ray diffraction (XRD) and the Scanning Electron Microscopy (SEM) and also the Atomic-force microscopy (AFM).

The addition of silver nanoparticles by mixing of a certain percentage from it with the mixture of the bilateral system at the construction of (53% A) plays an important role in the changing of the electrical properties of the bilateral system mixture, for this reason the silver nanoparticles has been chosen in this research to study the effect of adding it to the mixture of the bilateral system, on the electrical properties of the mixture.

We noticed through the LCR meter an increasing of the electrical conductivity of the mixture by the existence of silver nanoparticles in a concentration of (53% A).

**Key words:** liquid crystal, silver nanoparticles, electrical properties, X-ray diffraction, Atomic force microscope.

### Introduction

#### Liquid crystal

Liquid crystalline molecules are 'soft materials', representing special states of matter (also called the fourth state of matter) which is recognized by its long range order (as in crystals) and mobility (as in liquid)<sup>(1)</sup>. The matter in general, has three distinct states: solid, liquid, and gas<sup>(2)</sup>. The differences between these three states can be attributed to the temperature of the substance. Temperature is a

measure of the randomness of the molecules and therefore the higher the temperature is the less order they exist. Increasing temperature will cause the transition from a solid to a liquid and then to a gas<sup>(3)</sup>. Liquid crystals are substances that exhibit a phase of matter that has properties between those of a conventional isotropic liquid, and those of a solid crystal<sup>(4)</sup> fig (1).

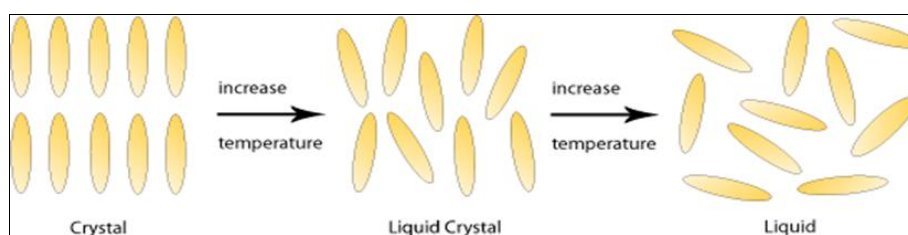


Figure (1): Alignment of the molecules for solid, liquid crystal and liquid phases

Most liquid crystal compounds exhibit polymorphism, or a condition where more than one phase is observed in the liquid crystalline state. The term mesophase is used to describe the "subphases" of liquid crystal materials. Mesophases can be characterized by the type of ordering that is present and they are formed by changing the amount of order in the sample, either by imposing order in only one or two dimensions, or by allowing the molecules to have a degree of translational motion<sup>(5)</sup>. There are two main types of liquid crystals: Thermotropic and lyotropic liquid crystals<sup>(6)</sup>.

There are many types of liquid crystal states, depending upon the amount of order in the material. The main types of liquid crystal phases:

- Nematic phase

This is the most liquid like structure in which, contrary to isotropic liquids, one or two molecular axes are oriented parallel to one another resulting in an orientational longrange order and short positional order. Molecules can rotate by both the axes, the molecules have several possibility of intermolecular mobility. Because of the high mobility, the nematic phases have low viscosities. They are anisotropic with respect to optical properties, viscosity, electrical and magnetic susceptibility, electrical and thermal conductivity<sup>(7-8)</sup>.

- Smectic phase

The smectic state is another distinct mesophase of liquid crystal substances<sup>(9-10)</sup>. The smectic phases,

which are found at lower temperatures than the nematic, form well-defined layers that can slide over one another like soap. The smectics are thus positionally ordered along one direction "smectic", there are many different types of smectic phases according to the chronological sequences of the detection that smectic phases have been designated with code letters A, B, C...M<sup>(11)</sup>. The most important ones are smectic A (SmA), smectic C (SmC) and smectic C\* (SmC\*).

- Cholesteric phase

The cholesteric (or chiral nematic) liquid crystal phase is typically composed of nematic mesogenic molecules containing a chiral center which produces intermolecular forces that favour alignment between molecules at a slight angle to one another. This leads to the formation of a structure which can be visualized as a stack of very thin 2-D nematic-like layers with the director in each layer twisted with respect to those above and below. In this structure, the directors actually form in a continuous helical pattern about the layer normal as illustrated by the black arrow in the following figure and animation. The black arrow in the animation represents director orientation in the succession of layers along the stack<sup>(12,13)</sup>.

- Columnar phase

Disk-shaped mesogens can orient themselves in a layer-like fashion known as the discotic nematic phase. If the disks pack into stacks, the phase is called a discotic columnar. The columns themselves may be organized into rectangular or hexagonal arrays<sup>(14)</sup>.

#### Binary system of liquid crystal

Liquid crystal materials for device applications are mostly mixtures because no single compound fulfils all the criteria. Mixing many compounds enables us to adjust the properties such as temperature range, electric permittivity, viscosity, birefringence, elastic constants etc. So the study of mixtures of liquid crystalline compounds is a subject of considerable interest. Generally a smectic phase is induced in binary mixtures of nematogenic compounds, one has terminal polar group and the other has terminal nonpolar group. In some cases, however, induced smectic phases have been observed when both the compounds have strong polar end groups or both the compounds have weakly polar end groups<sup>(15)</sup>.

#### Silver nanoparticles

Silver nanoparticles are being mass produced and utilized in hundreds of commercially available products (e.g., biomedical devices, water and air filters, food ware, electronic appliances, cosmetics, clothing, and numerous household products) due to their broad-spectrum antimicrobial properties and lower propensity to induce microbial resistance than other antibiotics<sup>(16,17)</sup>. In addition to products exploiting their antimicrobial properties, silver nanoparticles are also widely used in catalysis, optics and other areas due to their unique size-dependent optical, electrical and magnetic properties<sup>(18)</sup>.

The widespread use of silver nanomaterials has the potential to adversely affect human and ecosystem health. Silver nanoparticles may be released to the environment directly from products containing silver nanoparticles, such as colloidal silver medicine<sup>(19)</sup>.

In this paper, we aim to present and review snapshots of our recent research carried out on emerging applications of LCs, particularly focusing on the development of new applications based on a combination of LCs and functional nanomaterials, such as, silver nanoparticles. In addition, we will briefly discuss the permittivity and the connectivity of the binary system mixture with and without silver nanoparticles.

## Experimental

### Chemicals

p-chloro aniline, p-hydroxy benzaldehyde and Glacial acetic acid were obtained from Sigma-aldrich and p-bromo aniline obtained from Hopkin & Williams, ethanol abs. from J.T. Baker, while 1-Hexanol from Riedel- DE HAEN, Sodium nitrate was obtained from Romil, hydrobromic acid and Hydrochloric acid were available from BDH. Sulfuric acid was obtained from Biosolve. Silver nitrate was obtained from Degussa, and 4-nitrophenyl 4-(octyloxy) benzoate it was prepared and obtained from Halle University /department of chemistry.

### Instruments

All infra-red spectra of organic compounds were recorded in (Shimadzu, FT-IR 8300). Thermo grams were obtained using Differential scanning calorimetry (DSC) STA PT-1000. The textures of mesophases were studied with polarized optical microscope model BEAM rmm-7t equipped with automatic photomicrographic system model PMIOSP.. The prepared nanoparticles was characterized by x-ray diffraction using (Shimadzu – XR – 6000) device with Nickel - Copper filter for the x-ray radiation (Cu K $\alpha$ ,  $\lambda = 1.5406 \text{ \AA}$ ). Atomic Force Microscope (AFM) type PHYWE was used to study the surface of the nanoparticles. LCR Electronic Test Device is used to measure the Inductance (L), Capacitance (C), and Resistance (R) of a component. The electric properties are measured by using LCR (HEWLETT. PACKARD) device.

### Preparation of organic compounds:

#### Preparation of n-hexyl bromide<sup>(20)</sup>

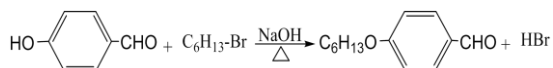
To 100 mL of 48% hydrobromic acid contained in a 250 mL round bottomed flask, 12.5 mL of concentrated sulfuric acid was added in portions with shaking and cooling in cold water (some hydrogen bromide may be evolved). A 1.5 mole of n-hexanol was added, followed by 12.5 mL of concentrated H<sub>2</sub>SO<sub>4</sub> in several portions. The reaction mixture was heated under reflux until the appearance of two layers. During this period the formation of n-hexyl bromide was almost completed and two layers were formed. Allow the contents of the flask to cool, remove the condenser and separate the two layers with separation funnel, discard the aqueous layer, the

organic layer was washed 3 times with an equal volume (1:1) of 10% HCl and water, and then the organic layer was separated and washed with an equal volume of 10% sodium bicarbonate solution and water. Separate the water as completely as possible and dry with 2-3 g of anhydrous calcium chloride. Filter the dried product through a small funnel supporting a fluted filter paper to give n-hexyl bromide.



#### Preparation of p-hexyloxy benzaldehyde<sup>(20)</sup>

In 100 ml round bottom flask p-Hydroxy benzaldehyde (5 gm, 0.0409 mole) was dissolved in 25 ml absolute ethanol then added (1.63 gm) of NaOH dissolved in ethanol and let to stirred with heat for 15 min. followed by (0.0409 mole) of P-n-hexyl bromide. The reaction mixture was heated gradually under reflux. After the reflux time completed depending on TLC, the product separated with separation funnel using water and ethyl acetate. Two layer was formed, discard the aqueous layer, the solution product was distilled to remove ethyl acetate and dried with calcium chloride. The solution of p-n-hexyloxy benzaldehyde was filtered and protected.



#### Preparation of N-(4-subst.phenyl)-1-(4-(hexyloxy)phenyl) methanimine

P-subst. aniline (0.0097 mole) was dissolved in 10 ml absolute ethanol then added (0.0097 mole) of p-(n-hexyloxy benzaldehyde) with 3 drop of glacial acetic acid. The reaction mixture was heated under reflux for 3h and after the time of reflux completed,



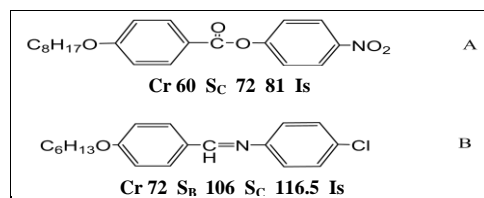
#### Preparation of binary mixtures

The binary mixtures are composed of:

(A) 4-nitrophenyl 4-(octyloxy)benzoate

(B) N-(4-chlorophenyl) - 1 - (4 - (hexyloxy) phenyl) methanimine

The components have the following structural formula:



The mole fraction of two compounds were calculated according to the following equation :

$$X\% = \frac{n_1}{n_1 + n_2} \dots\dots\dots (2.3)$$

depending on TLC. Allowed the reaction mixture to cool then the solid product was filtered and washed with cold ethanol and dried. The product was recrystallized from ethanol. Yield, recrystallization solvents and melting points of compounds (sch2-sch6) were listed in table (1).

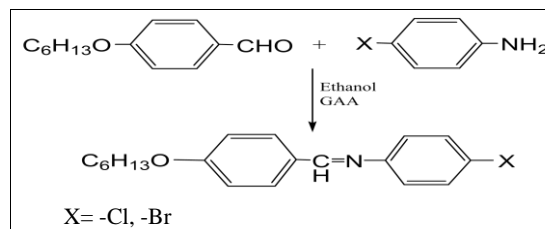


Table 1: Yield, recrystallization solvents and melting points of compounds (sch2, sch6)

Compound No.	Molecular Formula	-x	Yield	M.P.°C
Sch2	C <sub>19</sub> H <sub>22</sub> ONCl	-Cl	90%	72
Sch6	C <sub>19</sub> H <sub>22</sub> ONBr	-Br	94%	65

#### Preparation of silver nanoparticles<sup>(21)</sup>

A Solution of silver nitrate (1600 ml, 5 gm) was boiled in beaker 2500 ml then solution of tri-sodium citrate (250ml, 9 gm) was added slowly, drop by drop and kept the temperature between (95-100)°c with vigorous stirring. It was heated until the color of solution changed into (yellowish brown) and the silver nano particles began precipitate on the beaker wall like a mirror. After the end of the addition, the reaction mixture was cooled to room temperature and the product was collected in the solution and left to settle then put in ultra-sound device for 10 min. The following equation explains the reaction:

X = A% (mole fraction)

The n is expressed by Equation :

$$n = \frac{Wt}{M.Wt} \dots\dots\dots (2.4)$$

The weighed compounds were melted and mixed in the isotropic phase to obtain a homogenous mixture and let to cool and recrystallize, this process is repeated for three times. The obtained solid was finally ground and used for determining transition temperatures, by using polarizing microscope fitted with hot stage<sup>(22)</sup>.

The melting points and a mole fractions with different values of the binary and mixtures are shown in Table(2).

**Table 2: Melting points and a mole fraction of the binary mixtures system**

Mole % A	M.p (C°)
A	44.4
B	53.2
100	44.4
85	32.6
80	32.1
75	31.1
70	32
65	31.5
50	31.2
40	28.7
25	33.6
20	34.4
17.5	35.7
15	36.5
0	53.2

**Preparation of binary mixture with silver nanoparticle**

Silver nanoparticles (0.250g) were mixed with 0.5 g of mixture { (A) 4-nitrophenyl 4-(octyloxy) benzoate and (B) N-(4-chlorophenyl)-1-(4-(hexyloxy) phenyl) methanimine} and dissolved in ethanol (20mL). The mixture was homogenized with the Ultra- sound device for 15minutes. Then it was left at room temperature for 24 h .The liquid phase was separated from residual at the bottom of the beaker and the solvent was evaporated.

**Table 3: silver nanoparticles weight in the Binary and mixture**

Mixtures LC with nanoparticle	Wt of nanoparticle (g)	Wt of LC (g)
Binary(53%A) + silver nanoparticales	0.250	0.500

**Dielectric constant values measurements <sup>(23)</sup>**

The dielectric parameters as a function of frequency are described by the complex permittivity.

$$\epsilon^*(\omega) = \epsilon'(\omega) - \epsilon''(\omega) \dots \dots (2.1)$$

$\omega$  is the angular frequency

$$\omega = 2\pi f \dots \epsilon \dots (2.2)$$

$f$  is the applied frequency. When the real part  $\epsilon'$  and imaginary part  $\epsilon''$  are the components for the energy storage and energy loss respectively, in each cycle of the electrical field.

The measured capacitance  $C$  was used to calculate the dielectric constant,

$\epsilon'$  using the following expression :

$$\epsilon' = \frac{C d}{\epsilon_0 A}$$

Where  $d$  is the thickness between two electrodes (cell thickness)

$A$  is the area of the electrode

$\epsilon_0$  is permittivity of the space which equal to  $8.85 \times 10^{-12} \text{ F.m}^{-1}$

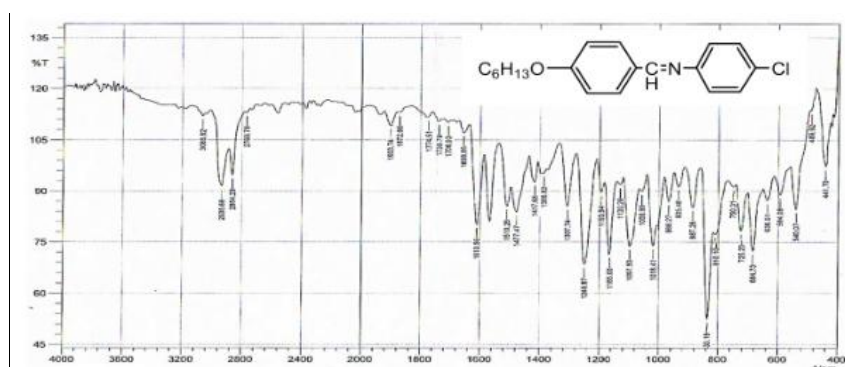
Whereas for dielectric loss  $\epsilon''$  and  $\tan\delta$  (tangenttheta):

$$\epsilon''(\omega) = \epsilon'(\omega) \cdot \tan \delta (\omega) \dots \dots (2.3)$$

The Ac conductivity ( $\sigma_{AC}$ ) can be calculated by the following equation:  $\sigma = \epsilon_0 \epsilon' \omega' \tan \delta \dots \dots (2.4)$

**Results and Discussion****FT-IR characterization****Characterization of N-(4-chlorophenyl)-1-(4-(hexyloxy) phenyl) methanimine**

This synthesized compound was identified by FT-IR spectrum <sup>(24)</sup>. The characteristic bands of N-(4-chlorophenyl)-1-(4-(hexyloxy)phenyl) methanimine are shown in Figure (2). The appearance of two bands at  $2935$  and  $2864 \text{ cm}^{-1}$  assigned to the asymmetrical and symmetrical stretching of C-H aliphatic respectively. The C=N bond appeared at  $1610$  and  $1575 \text{ cm}^{-1}$ . The appearance of typical absorption of C=C stretching in benzene rings was at  $1510$ ,  $1477 \text{ cm}^{-1}$ . The C-N stretch bond showed a single band at  $1249 \text{ cm}^{-1}$ . The C-O stretching bond showed a bands at  $1165$  and  $1097 \text{ cm}^{-1}$ . The C-H bending of the para disubstituted benzene appeared at  $968$ ,  $935$  and  $887 \text{ cm}^{-1}$ . The C-Cl bond showed absorption in  $835 \text{ cm}^{-1}$ .

**Figure (2): FTIR Spectrum of N-(4-chlorophenyl)-1-(4-(hexyloxy)phenyl) methanimine****Characterization of N-(4-bromophenyl)-1-(4-(hexyloxy) phenyl) methanimine**

This synthesized compound was identified by FT-IR spectrum <sup>(24)</sup>. The characteristic bands of N-(4-bromophenyl)-1-(4-(hexyloxy)phenyl) methanimine are shown in Figure (3). The appearance of two bands

at  $2951$ ,  $2921$  and  $2868 \text{ cm}^{-1}$  assigned to the asymmetrical and symmetrical stretching of C-H aliphatic respectively. The C=N bond appeared at  $1624$  and  $1602 \text{ cm}^{-1}$ . The appearance of typical absorption of C=C stretching in benzene rings was at  $1508$ ,  $1471 \text{ cm}^{-1}$ . The C-N stretch bond showed a

single band at  $1303\text{ cm}^{-1}$ . The C-O stretching bond showed a bands at  $1249$  and  $1165\text{ cm}^{-1}$ . The C-H bending of the para di-substituted benzene appeared

at  $1022,993$  and  $883\text{ cm}^{-1}$ . The C-Br bond showed absorption in  $835\text{ cm}^{-1}$ .

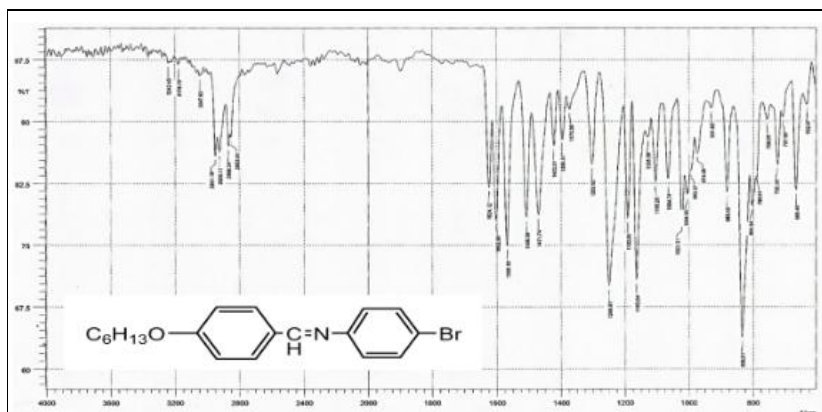


Figure (3): FT-IR spectrum of N-(4-bromophenyl)-1-(4-(hexyloxy)phenyl) methanimine

### DSC characterization

#### Liquid Crystalline Properties of N-(4-chlorophenyl)-1-(4-(hexyloxy)phenyl) methanimine

The DSC Thermogram of compound (sch2) showed two transitions peaks in figure (4). The first peak represented the transition temperature from crystalline phase to smectic C phase at  $81.3^\circ\text{C}$ , and the other peak represented the transition temperature from smectic C to smectic A phase to at  $88.4^\circ\text{C}$ .

The optical observation was performed with the hot-stage polarizing microscope of N-(4-chlorophenyl)-1-(4-(hexyloxy)phenyl) - methanimine. The transition temperatures were recorded for crystalline phase to smectic C phase at  $82^\circ\text{C}$ . In further heating, the Smectic C phase was converted into Smectic A phase  $102^\circ\text{C}$  (Figure5). In further heating the isotropic phase appeared at  $108^\circ\text{C}$ .

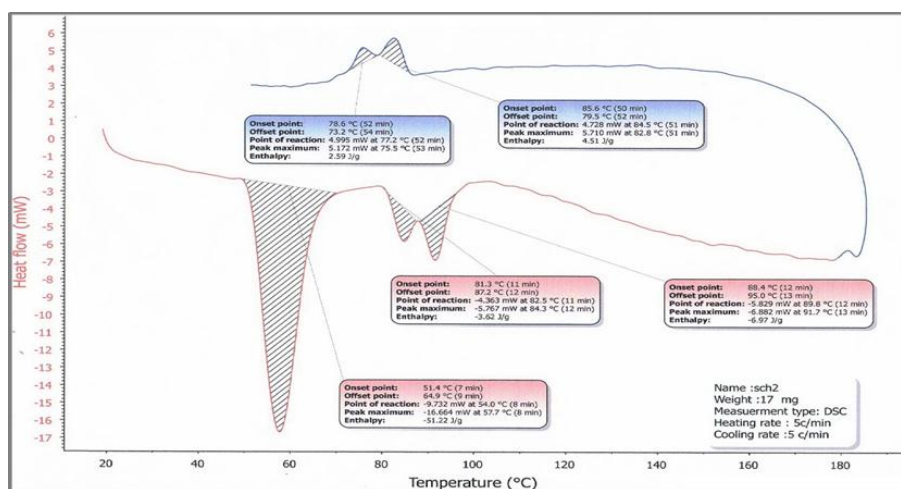


Figure 4: The DSC thermo gram of trace for sch2

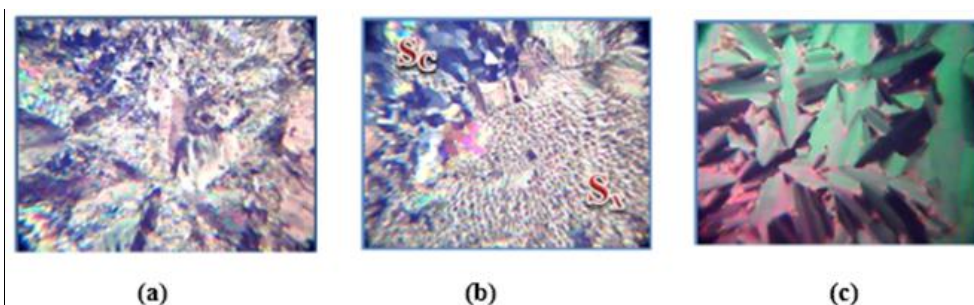


Figure 5: (a) Smectic C texture at  $82^\circ\text{C}$  (b) Smectic C phase transition to Smectic A phase at  $102^\circ\text{C}$  (c) Smectic A texture with cooling at  $84^\circ\text{C}$

**Liquid Crystalline Properties of N-(4-bromophenyl)-1-(4-(hexyloxy)phenyl) methanimine**

The DSC Thermogram of compound (Sch6) showed one transitions peak in figure (6). This peak represented the transition temperature from crystalline phase to smectic A phase at 96.6

The optical observation was performed with the hot-stage polarizing microscope of N-(4-bromophenyl)-1-(4-(hexyloxy) phenyl) methanimine. The transition temperatures were recorded for crystalline phase to smctic A at 97°C, on further heating the isotropic phase appeared at 122.2 °C (Figure 7).

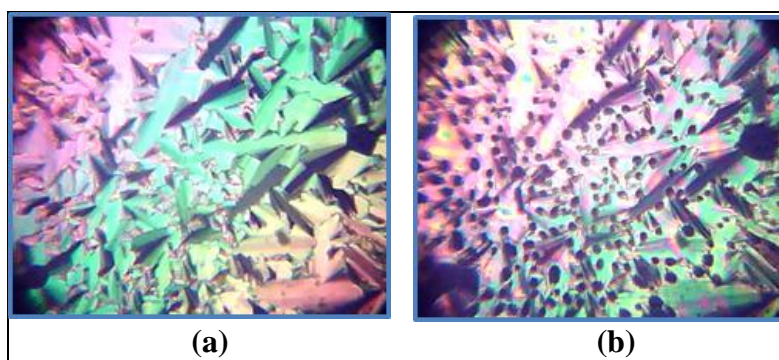
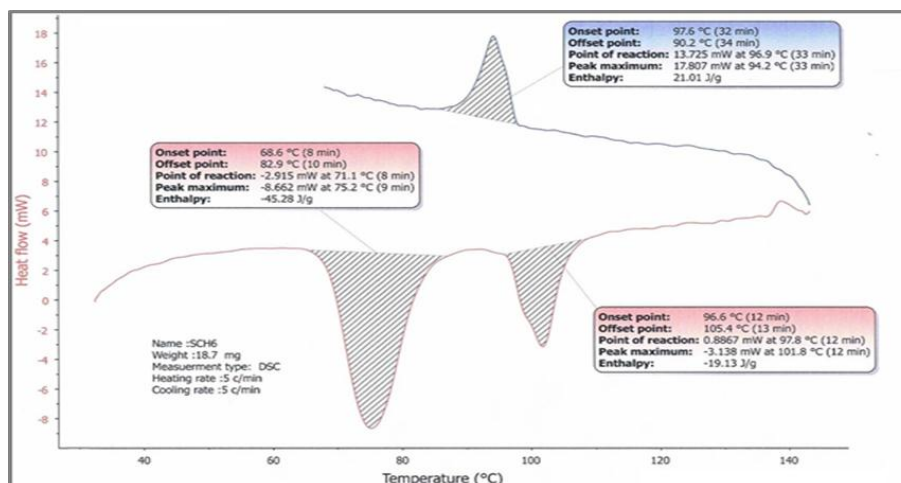


Figure 7: (a) Smectic A texture at 97 °C (b) Smectic A phase transition to isotropic phase at 122.2 °C

Table 4: Transition temperatures obtained from hot-stage microscopy of the compounds (sch2-sch6).

Compound No.	-x	Transition	T °C
Sch <sub>2</sub>	-Cl	Cr → S <sub>c</sub>	82
		S <sub>c</sub> → S <sub>A</sub>	102
		S <sub>A</sub> → I	108
Sch <sub>6</sub>	-Br	Cr → S <sub>A</sub>	97
		S <sub>A</sub> → I	122.2

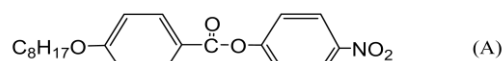
**Liquid Crystalline Properties and Characterization of mixtures Binary systems**

The binary mixtures are composed of two compounds:

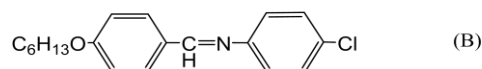
(A) 4-nitrophenyl 4-(octyloxy)benzoate (Dr<sub>1</sub>)

(B) N-(4-chlorophenyl)-1-(4-(hexyloxy) phenyl) methanimine (sch<sub>2</sub>)

The components have the following structural formula:



Cr 44. S<sub>x</sub> 53.2 N 59.9 Is



Cr 63.3 S<sub>c</sub> 78.4 S<sub>x</sub> 86.2 Is

Liquid crystalline properties of binary mixtures were studied using hot-stage polarized microscope to determine the transitions points between the phases, where different molar fractions values are taken as necessary cases of the diagnosis.

The Table (5) shows the binary mixture systems between (A) with an ester linking group as a core group, alkoxy terminal group and nitro non-polar group and (B) with Schiff base linking group as a core group and with alkoxy terminal groups and chloro polar group, this shows a concave down curve mesophase smectic x and nematic- isotropic transition temperatures. Figure (8) showed a

homogenous enantiotropic nematic phase, with wide concentration area (0-100% of A).

Figure (8) showed binary mixture system which revealed the presence of the eutectic transition temperature Cr → SmX (29.3 °C) SmX → N (34 °C) N → I (66.6 °C) transition at (respectively at the concentration region 53% A (mixture).

**Table 5: Transition temperatures(°C) of mixtures binary system phases.**

Mol % A	Cr	SmC	SmX	N	IS
A 100%	•	44.4	-	53.2	59.9
B 0%					
85	•	32.6	-	40.8	62.3
80	•	32.1	-	39.2	62.9
75	•	31.1	-	37.8	63.4
70	•	31.8	-	37.4	61.5
65	•	31.5	-	36.3	62.9
53	•	29.3	-	34	66.6
50	•	29.8	-	34.1	67.1
40	•	28.7	-	38.5	67.1
25	•	33.6	-	53.3	67.7
20	•	34.4	-	62.1	73.8
17.5	•	35.7		70.5	74
15	•	36.5	63.6	-	76.2
A 0%	•	53.3	78.4	-	86.2
B 100%					

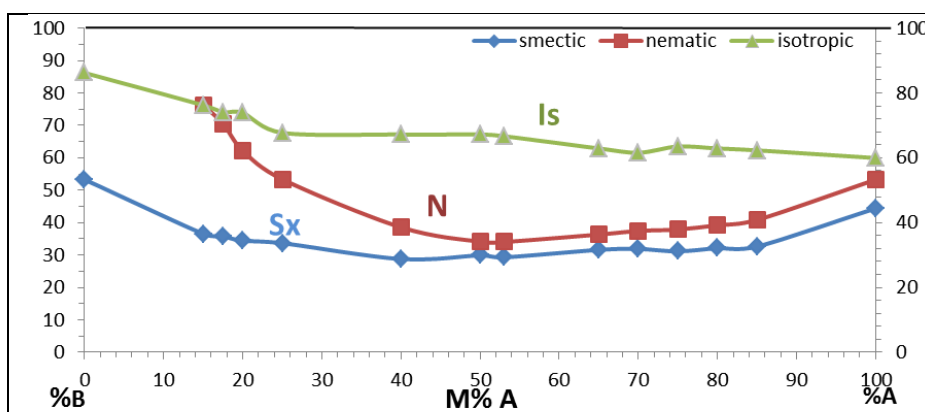


**Figure 8: Binary system mixtures of (A) and (B) transition temperature**

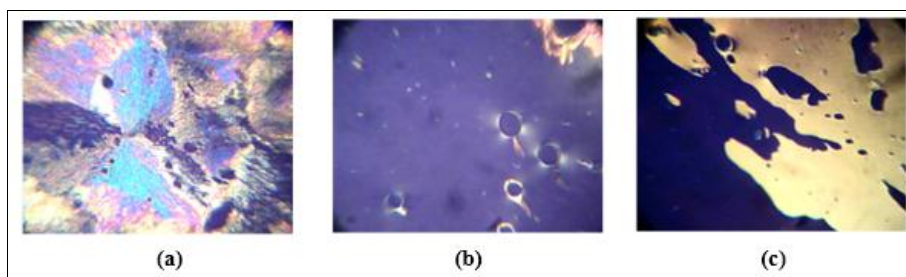


**Figure 9: (a) Transition from crystalline phase to smectic x phase of the binary system 53%A at 29.3 °C  
(b) Nematic homeotropic phase of the binary system 53%A at 36 °C  
(c) Nematic homeotropic phase of the binary system 53%A By pressing on the slide at 36 °C**

The eutectic point at 53% A was studied. The thermal behavior of this concentration was with DSC .Figure (10) showed two transition temperatures, the first one was at 33.6°C, and belong to the transition from

crystal solid to S<sub>x</sub> phase. The second transition showed the transition at 70.9°C from S<sub>x</sub> to nematic homeotropic phase.

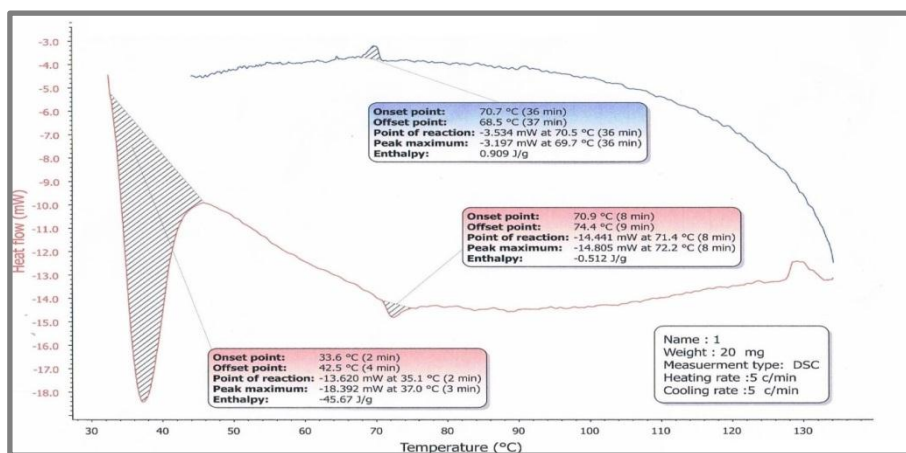


Figure 10: DSC thermogram of mixtures binary system (53%A)

**Nanoparticles characterizing**

**X-Ray Diffraction Studies of Silver nanoparticles**

The x-ray diffraction pattern of silver nanoparticles (figure 11) exhibit major three peaks at 38.12, 44.29 and 64.44 and show an inner layer spacing approximately 2.35848, 2.04347 and 1.44459, respectively without impurity peaks. This indicates the formation of pure silver nanoparticles. From Debye Scherrer equation, the particles size of silver nanoparticles was found 37.82 nm. Appearance of the XRD peaks (Figure 11) corresponding to product particles demonstrates typical nature of crystalline silver (JCPDS Card no. 89-3722)<sup>(25-26)</sup>. The size of the nanoparticles were calculated with the help of Debye

Scherrer formula to calculate particle (crystalline) size

$$D = \frac{K\lambda}{\beta \cos \theta}$$

Where;

D is the crystallite size,  $\lambda$  is the wavelength of the X-ray radiation ( $\text{CuK}\alpha = 0.15406 \text{ nm}$ ), k is a constant taken as 0.94,  $\theta$  is the diffraction angle and B is the line width at half maximum height. This is the generally accepted method to estimate the mean crystalline size of nanoparticles. The size of silver nanoparticles were 37.82 nm respectively.

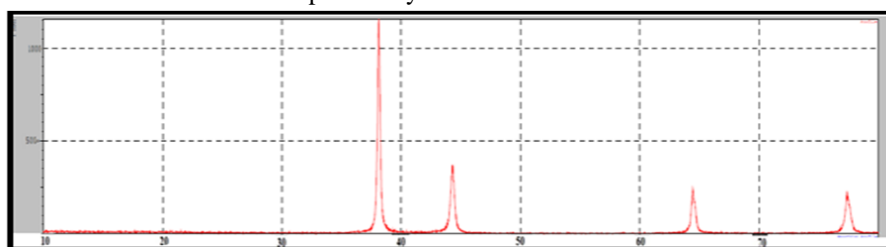


Figure (11): X-Ray Diffraction of silver nanoparticles Topography of the nanoparticles characterization with AFM and SEM

**Atomic Force Microscopy AFM**

The type of the nanoparticle was investigated with AFM. The AFM pictures of the samples were analyzed and slightly modified. Raw pictures of the topography are shown in figure (12) for silver nanoparticles.

It is important to study the topography of the materials in nanoscale and to know the morphology and surfaces for the nanoparticles. As far as AFM investigation of pure silver nanoparticles is concerned, figure (13) shows that the maximum height 47.9 nm and the height of detected region was 13.88 nm. On the other hand, the area was 372 nm. This indicates the pure silver nanoparticle prepared in nanoscale.

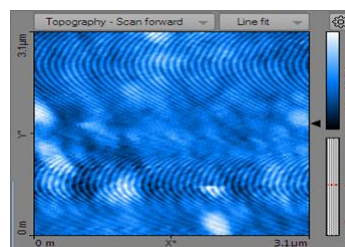


Figure (12): Topography-Scan for the single nanoparticles Ag

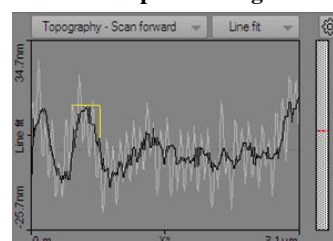


Figure (13): cross section of single nanoparticles Ag

**3.4.2.2 Scan electronic Microscopy SEM**

Figure (14) represented the SEM of the silver nanoparticles. The measurements were made the scan

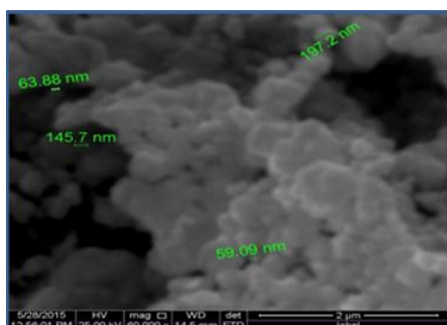
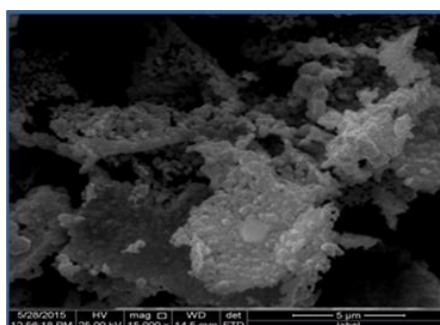


Figure (14): SEM of Ag nanoparticles in dry situation



by the micro scale, to show the accumulation of the nanoparticles in dry situation.

**Electrical Properties of liquid crystals binary system:**

The change of liquid crystal texture was observed in the presence of the AC electric current. The observation was also for the mixtures with and without nanoparticles.

The figures (15) and (17) represented regular textures of the binary mixture with and without nanoparticles as mentioned under the pictures. The presence of the AC electric current made evident deformations in the textures of the investigated samples, figures (16) and (18).

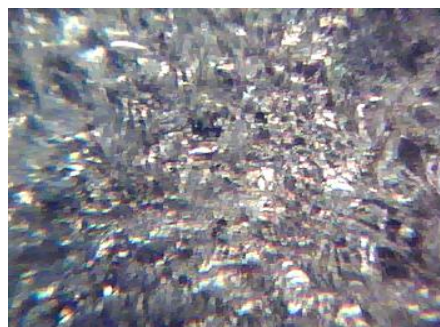


Figure (17): Binary mixture at (53%A) with Nano at (65°C) and without electric current



Figure (15): Binary mixture at (53%A) without Nano at (74°C) and without electric current

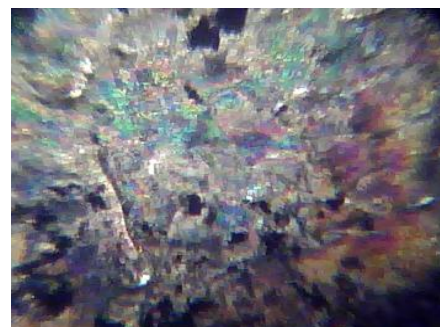


Figure (18): Binary mixture at (53%A) with Nano at (65°C) and with electric current

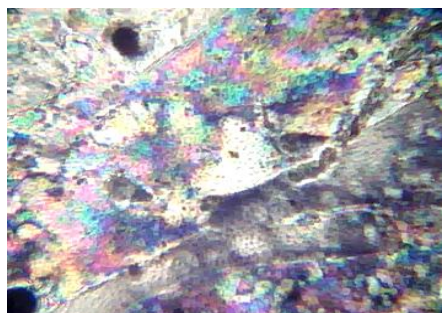


Figure (16): Binary mixture at (53%A) without Nano at (74°C) and with electric current

**Dielectric permittivity**

Each group showed the results of binary system measured in 400 hz and 1000hz. The figures were depicted the real, imaginary-permittivity and the Ac conductivity of the measurements. These measurements were carried out in binary (53%A) pure at the eutectic point concentration with the transition temperatures of Cr-Sx (29.9°C), Sx-N (34°C), N-I (66.6°C).

The figures of group one (19) showed the behavior of pure liquid crystalline mixtures (without nanoparticles) of binary at the eutectic point concentration (53%A) the real and imaginary permittivity ( $\epsilon'$  and  $\epsilon''$ ) was measured in the smectic, nematic and isotropic phase. The values of  $\epsilon'$  appeared at 400Hz higher than that value at 1000Hz. This means that the ability to store electric energy is more than loss at frequency of 400Hz. The values of  $\epsilon'$  and  $\epsilon''$  decreased as temperature increased.

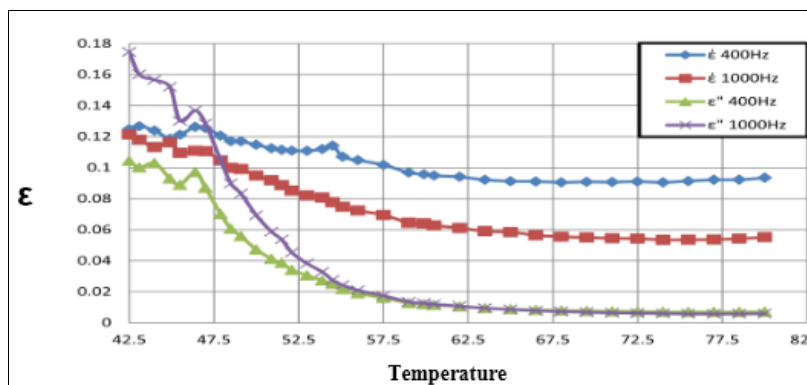


Figure (19): Pure binary mixtures 53%A permittivity 400 & 1000 hz

The figure (20) illustrated the behavior of  $\epsilon'$  and  $\epsilon''$  in binary liquid crystalline mixture system with silver nanoparticles at the eutectic point concentration (53%A). The measurements were taken in smectic, nematic and isotropic phase.

The  $\epsilon'$  shows higher values at the 400Hz than at 1000Hz in binary system was decreased with

increased of the temperatures. From this, we find that the ability to store electric energy has increased in the presence of silver nanoparticles at the frequency of 400 hz .

The values of  $\epsilon''$  of binary systems showed higher values at 1000Hz than at 400Hz and decreased with the increase of the temperatures.

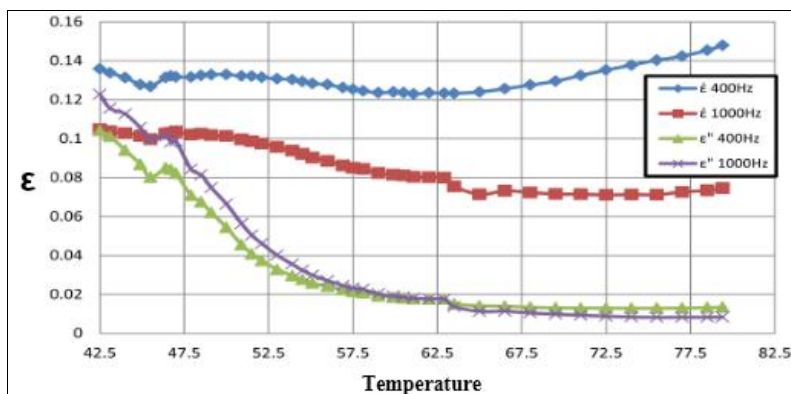


Figure (20): Binary mixture 53%A with silver nanoparticles permittivity 400&1000 Hz

The interpretation of the dielectric properties can be carried out through the differences in orientational order in the phases. This will affect the internal field factors and short range dipole - dipole interactions. Polar messages dipole - dipole association is an important contributor to the physical properties of liquid crystal phases, and this is particularly important in smectic and nematic phases, where the order can affect the dipole- dipole correlation factors<sup>(27)</sup>.

This may lead to the conclusion that the dipole moments exhibit parallel correlations with electric field direction liquid crystalline phases of the mixtures. Within the smectic and nematic phases, the permittivity practically approximates little differences or constant. These values were in agreement with the values reported for the pure nematogens as well as in binary mixtures<sup>(28-29)</sup>. Figure (19) depicts the variation of real part of dielectric permittivity ( $\epsilon'$ ) with two frequencies at eutectic point concentration at different temperatures. At 400 and 1000 Hz frequencies, permittivity attained higher values at low temperature, which diminished rapidly with temperature increasing. This is reasonable since – in

the low temperature region – the liquid crystals molecules have a low kinetic energy, providing thus sufficient time to permanent and induced dipoles to align themselves according to the applied field, leading to enhanced polarization. Enhanced values of ( $\epsilon'$ ) especially at low temperatures can be attributed interfacial polarization, and/or electrode polarization. Electrode polarization is related to the buildup of space charges at the specimen-electrode interfaces and is characterized by very high values of both real and imaginary part of dielectric permittivity<sup>(30,31)</sup>.

#### Conductivity

The presence of the nanoparticles also affects the conductivity of the pure liquid crystals mixtures. The conductivity of the pure and doped mixtures has also been measured at two different frequencies. The variation of the conductivity with the change in temperature at 400 Hz and 1000 Hz has been shown in figures (21) and (22). The variation of conductivity of the doped binary system is not similar to both the frequencies due to the symbioses of the dispersed nanoparticles and the free ions existing in the liquid crystals material. The presence of nanoparticles rouses the motion of the free ions near the 1000 Hz

frequency while it is less effective at lower frequency (i.e. near 400Hz). The value of conductivity for the mixture doped with nanoparticles system was almost between (2-29) times higher compared with pure mixtures. The conductivity at 400 and 1000 Hz for the pure mixtures decreases slightly with the increase in temperature whereas for the nanoparticles

dispersed mixtures, the conductivity increases nonlinearly with the decrease of temperature. The conductivity of liquid crystals mixtures doped with nanoparticles is higher than the pure binary. Further existence of silver nanoparticles will increase the number of interfaces and effect on the (percolation threshold) caused a conducting network and leads to increase the electrical conductivity<sup>(32)</sup>.

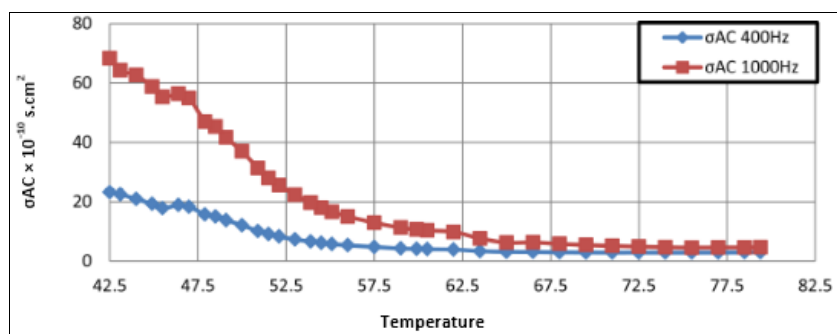


Figure (21): Binary mixture 53%A pure conductivity 400&1000 hz

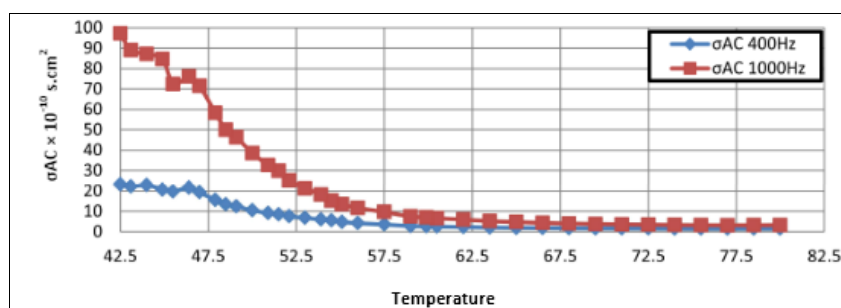


Figure (22): Binary mixture 53%A with silver nanoparticle conductivity 400&1000 hz

## Conclusion

The binary mixture system was shown enantiotropy smectic phase and homeotropic nematic phase at temperatures less than they were before the liquid crystalline compounds incorporated into the binary mixture system.

1. The conductivity and the real and imaginary permittivity increased with the decrease of temperatures, and this is useful in liquid crystal display (LCD).

## References

1. A. Puzari, Liquid Crystalline Organic Compounds and Polymers as Materials, 37, pp.95-124, 2011.
2. R.B. Seymour and C.E. Carraher, "Polymer chemistry: An Introduction", A series of text books, New York and Basel, Vol. 8, (1999).
3. W.H. Carothers, J. Amer. Chem. Soc., 51, 2548 (1929).
4. Reinitzer, F. Beitrage zur kenntniss des cholesterins. Monatsh, Chem. 1888, 9, 421–441 (in German Language).
5. R.J. Birgeneau, and J.D. Lister, J. Phys.(Paris), 39, 399 (1978).
6. D. Demus, Liquid Crystals, 5, 75,1989.
7. G.Gray, "Thermotropic Liquid Crystals", Wiley, New York, (1987).

2. The addition of silver nanoparticles reserved the texture of the nematic phase and kept it without change.

3. The conductivity of liquid crystals binary mixture system doped with silver nanoparticles is higher than the pure binary.

4. The silver nanoparticles shown a good data in low frequency (400 hz) for real  $\epsilon'$  and imaginary  $\epsilon''$  permittivity and conductivity this may indicated a useful in liquid crystal mixture doped with nanoparticles.

8. P. J. Collings, Liquid Crystalline Materials, In Kirk-Othmer Encyclopedia of Chemical Technology, 4th edn., Wiley, New York, Vol. 15 , 372-409 (1995).
9. D.Demus, J.Goodby, G.w. Gray, H.W. Spiess, and V. Vill, "Handbook of Liquid Crystals", Vol. 1-3, Wiley VCH, (1998).
10. H. Sackmann, Liquid Crystals, 5, 43(1989).
11. P.J. Flory, Proc. R. Soc. London Ser. A, 73,234,(1956).
12. A. Yu. Bobrovsky, N. I. Boiko and V. P. Shibaev, Liq. Cryst., 27(2), 123 (2000).
13. A. Bacilieri, U. Caruso, B. Panunzi, A. Roviello and A. Sirigu, Polymer, 41(17),6423-6430 (2000).

14. M.P. Allen and D. J. Tildesley, Simulations: "Computer simulation of liquids", Oxford University Press (1987).
15. S. D. Sarkar and B. Choudhury. Assam University Journal of Science & Technology: Physical Sciences and Technology. Vol. 5 Number II. 167-168, 2010. Study of binary mixtures of two liquid crystalline samples showing induced smectic phase.
16. Andrew D. Maynard<sup>1</sup>, Robert J. Aitken, Tilman Butz, Vicki Colvin, Ken Donaldson, Günter Oberdörster, Martin A. Philbert, John Ryan, Anthony Seaton, Vicki Stone, Sally S. Tinkle, Lang Tran, Nigel J. Walker & David B. Warheit. Safe handling of nanotechnology. Nature. 444(7117): p.267-269, 2006.
17. Marambio-Jones, C. and E.M.V. Hoek, A review of the antibacterial effects of silver nanomaterials and potential implications for human health and the environment. Journal of Nanoparticle Research JNR. 12(5): p. 1531-1551, 2010.
18. Rejeski, D., Nanotechnology and consumer products. 2009; Available from: [http://www.nanotechproject.org/publications/archive/nanotechnology\\_consumer\\_products/](http://www.nanotechproject.org/publications/archive/nanotechnology_consumer_products/).
19. Mueller NC., Nowack B., Exposure modeling of engineered nanoparticles in the environment. Environmental Science & Technology. 42(12): p. 4447-4453, 2008.
20. A. Vocal, "A Text Book of Practical Organic Chemistry", 5th edit. Longman, London, P 1000 (1998).
21. Basavaraj udapudi , Praveenkumar Naik, Sabiha Tabassum Savadatti, Rupali Sharma, Samprita Balgi. Ijpbs |volume 2| issue 3, 10-14|july-sept|2012|. Synthesis and characterization of silver nanoparticles.
22. J. Dave, M.R. Menon and P.R .Patel "Liquid crystalline behavior of structurally dissimilar mesogens in binary systems" University of Baroda. Proc. Indian ACAD. Sci.114 (3), p215, 2002.
23. A. Javed<sup>1</sup>, m. Akram<sup>2</sup>, and, m. I .shafiq "dielectric properties of cholesterol derivatives". University of the punjab. Rom. Journ. Phys.51 (7-8), p819–826, 2006.
24. Silverstian, "Spectroscopy chemistry", New York, 4th edition.
25. J. Rodriguez-Carvajal, Physica B 192, 55 (1993).
26. J. Rodrigues-Carvajal, "Win PLOTTR", Win PLOTTR user's guide, Laboratoire Leon Brillouin (CFA-CNRS), France, April (1999).
27. A.V. Koval'chuk, "Relaxation processes and charge transport across liquid crystal-electrode interface " J.Phys.Condens. Mater., 113(24),p10333-10345.
28. R Dabrowski & S .Urban, LiqCryst.24 , p583, 1998.
29. L. Bata & A. Buka, ActaPhysPolonica.54, p635, 1978.
30. Tsangaris G. M., Psarras G. C., Kouloumbi N.: Electric modulus and interfacial polarization in composite polymeric systems. Journal of Materials Science, 33,2027–2037 (1998). DOI: 10.1023/A:1004398514901 .
31. Psarras G. C., Gatos K. G., Karahaliou P. K., Georga S.N., Krontiras C. A., Karger-Kocsis J.: Relaxation phenomena in rubber/layered silicate nanocomposites. Express Polymer Letters, 1, 837–845 (2007). DOI: 10.3144/expresspolymlett. 2007. 116.
32. Yu Chao Li, Robert Kwok Yiu Li, and Sie Chin Tjong -Hindawi Publishing Corporation Journal of Nanomaterials Volume 2010, Article ID 261748, doi:10.1155/2010/261748 .

## دراسة تأثير اضافة دقائق الفضة النانوية في الخواص الكهربائية لنظام المزيج الثنائي للمركبات ذات الخواص البلورية السائلة

أسامة عبد إبراهيم حسن<sup>1</sup> ، عماد التكريتي<sup>1</sup> ، عصام عبدالكريم عبداللطيف<sup>2</sup> ، هناء كائن صالح<sup>1</sup>

<sup>1</sup>قسم الكيمياء ، كلية العلوم ، جامعة تكريت ، تكريت ، العراق

<sup>2</sup>قسم الكيمياء ، كلية التربية ابن الهيثم ، جامعة بغداد ، بغداد ، العراق

### الملخص

تأتي أهمية المركبات ذات الخواص البلورية السائلة من خلال استخدامها في الكثير من التطبيقات العملية، لذلك فإن دراسة خواصها الكهربائية ودراسة تأثير وجود الدقائق النانوية في خواصها الكهربائية بشكل خاص من الأمور المهمة أيضاً. في هذا البحث حُضرت عدد من المركبات العضوية وشُخصت هذه المركبات المحضرة باستخدام طيف الأشعة تحت الحمراء (FT-IR) ، ومجهر المسعر التفاضلي (DSC) والمجهر الضوئي المستقطب ، ومن ثم تم اختيار مركبين يمتلكان خواص بلورية سائلة وعمل مزيج من النظام الثنائي، وقد حصلنا من خلال ذلك على أقل درجة حرارة عند تركيز (53%A)، كما وقد شُخص هذا المزيج بواسطة مجهر المسعر التفاضلي (DSC) والمجهر الضوئي المستقطب. وحُضرت دقائق الفضة النانوية وتم تشخيصها بواسطة قياسات الأشعة السينية (XRD)، وقياسات المجهر الإلكتروني الماسح (SEM)، ومجهر القوى الذرية (AFM). إن إضافة دقائق الفضة النانوية عبر مزجها بنسبة محددة مع مزيج النظام الثنائي عند التركيز (53%A) يلعب دوراً مهماً في تغيير الخواص الكهربائية لهذا المزيج الثنائي؛ لذلك فقد أُختبرت دقائق الفضة في هذا البحث لدراسة تأثير إضافتها للمزيج على خواصه الكهربائية.

لقد لاحظنا من خلال قياسات LCR زيادة التوصيلية الكهربائية للمزيج الثنائي بوجود دقائق الفضة عند تركيز (53%A).

**الكلمات المفتاحية:** البلورات السائلة ، دقائق الفضة النانوية ، الخواص الكهربائية ، حيود الأشعة السينية ، مجهر القوى الذرية.